

On the treatment of ℓ -changing proton-hydrogen Rydberg atom collisions

D. Vrinceanu,^{1*} R. Onofrio,^{2,3} and H. R. Sadeghpour⁴

¹ *Department of Physics, Texas Southern University, Houston TX 77584, USA*

² *Dipartimento di Fisica e Astronomia “Galileo Galilei”, Università di Padova, Via Marzolo 8, 35131 Padova, Italy*

³ *Department of Physics and Astronomy, Dartmouth College, 6127 Wilder Laboratory, Hanover NH 03755, USA*

⁴ *ITAMP, Harvard-Smithsonian Center for Astrophysics, Cambridge MA 02138, USA*

Accepted XXX. Received YYY; in original form ZZZ

ABSTRACT

Energy-conserving, angular momentum-changing collisions between protons and highly excited Rydberg hydrogen atoms are important for precise understanding of atomic recombination at the photon decoupling era, and the elemental abundance after primordial nucleosynthesis. Early approaches to ℓ -changing collisions used perturbation theory for only dipole-allowed ($\Delta\ell = \pm 1$) transitions. An exact non-perturbative quantum mechanical treatment is possible, but it comes at computational cost for highly excited Rydberg states. In this note we show how to obtain a semi-classical limit that is accurate and simple, and develop further physical insights afforded by the non-perturbative quantum mechanical treatment.

Key words: cosmology: observations–primordial nucleosynthesis – ISM: abundances – atomic data

1 INTRODUCTION

The dynamics of atomic recombination and its impact on the cosmic background radiation are crucial to constrain variants of Big Bang models (Chluba, Rubiño-Martin & Sunyaev 2007; Chluba, Vasil & Dursi 2010). The recombination cascade of highly excited Rydberg H atoms is influenced by energy-changing (Vrinceanu, Onofrio & Sadeghpour 2014; Pohl, Vrinceanu & Sadeghpour 2008) and angular momentum-changing collisional processes (Pengelly & Seaton 1964 - PS64 thereafter; Vrinceanu, Onofrio & Sadeghpour 2012 - VOS12 thereafter), and is a major source of systematic error for an accurate determination of the recombination history. Moreover, primordial nucleosynthesis is studied by determining the He/H abundance ratio. This is obtained by determining the ratio of emission lines of He I and H I, and using the most accurate models for the recombination rate coefficients (Ferland 1986; Benjamin, Skillman & Smits 1999, 2002; Luridiana, Peimbert & Peimbert 2003; Izotov 2006, 2007).

Besides cosmology, recombination rate coefficients for hydrogen and helium are also important in studying radio emission from nebulae (Pipher & Terzian 1969; Brocklehurst 1970; Samuelson 1970; Otsuka, Meixner & Riebel 2011), and in the study of cold and ultracold laboratory plasmas (Gabrielse 2005). In particular, there is a pending puzzle in

the determination of elemental abundance and electron temperature in planetary nebulae, as optical recombination lines and collisionally induced lines provides significantly different values (Izotov 2006; García-Rojas & Esteban 2007; Nicholls, Dopita & Sutherland 2012; Storey & Sochi 2015).

Dipole ℓ -changing collisions $n\ell \rightarrow n\ell \pm 1$ between energy-degenerate states within an n -shell are dominant in the dynamics of proton-Rydberg hydrogen atom collisions, and have been addressed long ago by Pengelly and Seaton in the framework of the Bethe approximation in a perturbative framework (PS64). More recently, we examined (VOS12) the problem obtaining non-perturbative results for arbitrary $n\ell \rightarrow n\ell'$ energy-conserving transitions, including the dipole allowed transitions, which produce rate coefficients smaller compared with PS64. This results in the estimation of higher densities for available spectroscopic data, which is of relevance at least in cosmology as different H I emissivities are derived using the two models, with differences of up to 10% (Guzmán et al. 2016). This in turn impacts the precision required on the primordial He/H abundance ratio to constrain cosmological models.

The exact quantum expression obtained in VOS12 was complemented by a simplified classical limit transition rate that was in good quantitative agreement with the quantum rate and also with the results of Monte Carlo classical trajectory simulations for arbitrary $\Delta\ell$. For dipole allowed transitions, $\Delta\ell = \pm 1$, Monte Carlo computations in VOS12 predicted a finite cross section instead of a logarithmically di-

* E-mail: vrinceanud@tsu.edu

vergent one, due to a discontinuity in the classical transition probability at large impact parameters.

In a recent publication Storey & Sochi (2015) recommended that the PS64 rates should be preferred over the classical results in VOS12 due to how PS64 employed an *ad hoc* density-dependent cutoff procedure to treat the dipole-allowed angular momentum changing collisions. In a series of papers Guzmán et al. (2016, 2017); Williams et al. (2017) investigated the influence of differently calculated ℓ -changing rate coefficients in CLOUDY simulations of emissivity ratios, concluding that the quantum VOS12 treatment is more appropriate when modeling recombination through Rydberg cascades. In this note, we provide further validations and insights on our model and show how a slightly different classical limit is constructed to provide non-perturbative expressions that are uniformly consistent with the quantum behavior for all impact parameters. In this way, the deficiency of the classical transition rates discussed by Guzmán et al. (2016, 2017); Williams et al. (2017) is effectively eliminated.

2 PROTON-HYDROGEN ATOM COLLISIONS AT LARGE IMPACT PARAMETER

Consider an ion projectile with electric charge, in elementary units, of Z moving at speed v smaller or comparable with that of the target Rydberg electron $v_n = e^2/n\hbar$ in a state with principal quantum number n and angular quantum number ℓ . Results for collisions with proton are obtained by setting $Z = 1$. Even when the impact parameter b is larger than the size of the Rydberg atom, $a_n = n^2 a_0$, with n the principal quantum number and $a_0 = 0.53 \times 10^{-10}$ m the Bohr radius, the weak electric field created by the projectile lifts the degeneracy of the Rydberg energy shell and mixes angular momentum states within the shell. At the end of the slow and distant collision with the ion, the Rydberg atom is in a different angular momentum state with the same initial energy. Therefore collisions that change angular momentum, without any energy transfer, have extremely large cross sections and rate coefficients. The rate coefficient q of this process scales as $q_{n\ell \rightarrow \ell'} \sim n^4 / \sqrt{T} \Delta \ell^3$ (VOS12) with temperature T , and change in angular momentum $\Delta \ell = \ell' - \ell$.

Since the angular momentum changing collisions are most probable at large impact parameters it is safe to assume that the dipole term in the interaction energy dominates over the other multipolar contributions, which can be therefore neglected. Moreover, as the projectile has a much greater angular momentum than that of the target atom, it can be assumed that the projectile's angular momentum is conserved and the projectile moves along a straight line trajectory defined by the projectile position vector $\mathbf{R}(t)$. According to these assumptions, the Hamiltonian of the Rydberg electron contains a time-dependent interaction potential term given by

$$V(t) \approx -Ze^2 \frac{\mathbf{r} \cdot \mathbf{R}(t)}{|\mathbf{R}(t)|^3}, \quad (1)$$

where \mathbf{r} is the electron position. At extremely large impact parameter $b \gg n^2 a_0$ the interaction potential (1) may be treated as a perturbation and the collision can be treated in

the first Born approximation for the transition probability

$$\begin{aligned} P_{n\ell \rightarrow n\ell \pm 1}^{(B)} &= \frac{1}{\hbar^2} \frac{1}{2\ell + 1} \sum_{mm'} \left| \int_{-\infty}^{\infty} \langle n\ell' m' | V(t) | n\ell m \rangle dt \right|^2 \\ &= 3 \left(\frac{Ze^2 a_0}{\hbar b v} \right)^2 \frac{\ell_{>}}{2\ell + 1} n^2 (n^2 - \ell_{>}^2) \end{aligned} \quad (2)$$

where $\ell_{>} = \max(\ell, \ell \pm 1)$. This result has been obtained in the pioneering work PS64 and forms the basis for PS64 rate coefficient for angular momentum changing collisions. Although simple and easy to use, the expression (2) leads to a number of severe difficulties at smaller b . Various proposals were published attempting to improve the theory beyond the perturbation theory: close-coupling channel approximation (Bray & Stelbovics 1992), infinite level (Presnyakov & Urnov 1970), and rotating frame approximations (Bellomo 1998). This also stimulated experimental investigations, in which the redistribution of Na(28) Rydberg atom ℓ states in collisions with slow Na^+ ions was measured (Sun & McAdams 1993).

Specifically, the difficulties that stem from using perturbative solutions for the potential (1) are:

(i) The perturbative solution is derived from the matrix elements of (1) with respect to unperturbed states, and therefore only results for $\ell \rightarrow \ell \pm 1$ transitions can be obtained with this theory, as prescribed by the dipole selection rule.

(ii) The transition probability (2) diverges as $b \rightarrow 0$, violating $P_{n\ell \rightarrow n\ell \pm 1} < 1$, reflecting unitarity. This difficulty is handled in the PS64 formulation by introducing a cutoff impact parameter R_1 such that the probability for transitions at $b \leq R_1$ is exactly 1/2: $P_{\ell \rightarrow \ell \pm 1}^{(PS)}(v, b \leq R_1) = 1/2$. The justification for this adjustment was that for $b < R_1$, $P(b)$ is an oscillatory function with a mean value close to 1/2. This assumption is quite reasonable for collisions involving energy transfer, when the cutoff R_1 is about the size of the atom. However, the probability for angular momentum changing collisions are dominated by very large impact parameters ($b \gg n^2 a_0$) and probabilities for collision at small impact parameters are much smaller than 1/2. In order to address this difficulty an extension to PS64 method was recently proposed (Guzmán et al. 2017) in which the constant 1/2 is replaced with 1/4 (model PS-M in that paper). The overall trend of $P(b)$, as explained in the next sections, is to grow linearly with b . This is the reason why the PS64 rates are overestimated.

(iii) As $b \rightarrow \infty$, $P_{n\ell \rightarrow n\ell \pm 1}^{(B)} \sim 1/b^2$, leading to a cross section

$$\sigma_{n\ell \rightarrow n\ell'} = 2\pi \int_0^{R_c} P_{n\ell \rightarrow n\ell'} b db \quad (3)$$

which diverges logarithmically as $\log(R_c)$ when the cut-off parameter $R_c \rightarrow \infty$. The divergence of the cross section can be understood in the context of the dynamics of degenerate quantum systems, such as the ℓ -levels shell in a Rydberg atom. The transition between degenerate states under the influence of a perturbation that have non-zero coupling matrix elements is possible no matter how weak this perturbation is. The time scale governing transition probabilities is defined by the Rabi frequency, which for a degenerate system is given simply by $|V_{ab}|/\hbar$, where V_{ab} are the transition

matrix elements of the perturbation V between degenerate states a and b . Therefore, for weak electric fields, either produced during a very distant collision with an ion, or microfields generated by the surrounding plasma, the $\ell \rightarrow \ell \pm 1$ dipole transitions between Rydberg levels have rates proportional to the intensity of the perturbation.

3 EXACT NON-PERTURBATIVE TRANSITION PROBABILITY

By taking advantage of the symmetries in the problem, an exact non-perturbative solution for the Rydberg atom dynamics under the interaction potential (1) can be obtained (Vrinceanu & Flannery 2001a) and expressed as successive physical rotations, with direct interpretations both in quantum (Vrinceanu & Flannery 2000) and classical (Vrinceanu & Flannery 2001b) contexts. Like in other physical situations, for example the precession of a magnetic moment in magnetic field, the source of similarities between quantum and classical motions is the group of symmetry operations for the given system, which for the hydrogen atom is $SO(4)$.

The exact result for the non-perturbative transition probability is

$$P_{n\ell \rightarrow n\ell'} = \frac{2\ell' + 1}{2j + 1} \sum_{L=|\ell' - \ell|}^{2j} (2L + 1) \left\{ \begin{matrix} \ell' & \ell & L \\ j & j & j \end{matrix} \right\}^2 H_{jL}^2(\chi) \quad (4)$$

Here $\{\dots\}$ is Wigner's six- j symbol, and H_{jL} is the generalized character function for irreducible representations of rotations defined by

$$\begin{aligned} H_{jL}(\chi) &= \sum_m C_{jmL0}^{jm} e^{-2im\chi} \\ &= L! \sqrt{\frac{(2j+1)(2j-L)!}{(2j+L+1)!}} (2\sin\chi)^L C_{2j-L}^{(L+1)}(\cos\chi) \end{aligned} \quad (5)$$

where $C_{j_1 m_1 j_2 m_2}^{j m}$ are the Clebsch-Gordan coefficients and $C_n^{(a)}(\chi)$ are ultraspherical (Gegenbauer) polynomials. The effective rotation angle χ is

$$\sin\chi = \frac{2\alpha}{1 + \alpha^2} \left[1 + \alpha^2 \cos\left(\frac{\pi}{2} \sqrt{1 + \alpha^2}\right) \right]^{1/2} \sin\left(\frac{\pi}{2} \sqrt{1 + \alpha^2}\right) \quad (6)$$

with α a parameter that characterizes the dynamics of the ion projectile incoming at speed v

$$\alpha = \frac{3Zn\hbar}{2m_e v b} \quad (7)$$

This parameter can be expressed as the product of the Stark precession frequency and the collision time. Here m_e is electron mass.

The probability (4) eliminates all the difficulties associated with the perturbative expression (2) as it is not restricted to dipole transitions, it is well behaved in the $b \rightarrow 0$ limit, has simpler classical and semi-classical limits, as explained in the next sections, beyond the perturbative approximation.

The large $b \rightarrow \infty$ (or small $\alpha \rightarrow 0$) limit for the $\ell \rightarrow \ell \pm 1$ transition probability (4) can be obtained from the first $L = 1$ term in the summation and by observing that

$$\lim_{\alpha \rightarrow 0} H_{j1}(\chi) = \frac{2j+1}{3} \sqrt{j(j+1)} 4\alpha \quad (8)$$

and that the six- j symbol has a particularly simple form in this case

$$\left\{ \begin{matrix} \ell \pm 1 & \ell & 1 \\ j & j & j \end{matrix} \right\}^2 = \frac{L_>(n^2 - \ell_>^2)}{n(n^2 - 1)(4\ell_>^2 - 1)} \quad (9)$$

The result for the limit

$$\lim_{\alpha \rightarrow 0} P_{n\ell \rightarrow n\ell \pm 1} = \frac{4}{3} \frac{\ell_>}{2\ell + 1} (n^2 - \ell_>^2) \alpha^2 \quad (10)$$

is identical with the perturbative result (2).

Equation (4) can be efficiently implemented for the computation of approximation-free transition rates for angular momentum changing collisions for use in astrophysical models, beyond the PS64 result. However, for $n \gtrsim 100$, the direct summation becomes inefficient and it might lead to accumulation of truncation errors due to summation of large alternating sign numbers. For these cases, and also with the goal of obtaining more physics insight into this process, it is useful to investigate the limit $n \rightarrow \infty$ of (4). This can be done in two different ways, as explained in the next sections: one which applies for general transitions and impact parameters up to a critical value, and another one that applies only to dipole allowed transitions and very large b .

4 CLASSICAL LIMIT

The Bohr's correspondence principle asserts that quantum calculations tend to reproduce results obtained by using classical mechanics in the limit of large quantum numbers. In the case of the probability (4) this limit is obtained by transforming the summation into an integral and allowing quantum numbers to have continuous values,

$$\lim_{n \rightarrow \infty} P_{n\ell \rightarrow n\ell'} = 2\ell'n \int_0^1 \left\{ \begin{matrix} \ell' & \ell & L \\ j & j & j \end{matrix} \right\}^2 H_{jL}^2(\chi) d(L/n)^2 \quad (11)$$

The classical limit of Wigner's six- j symbol (Ponzano & Regge 1968) is given by $1/24\pi\sqrt{V_T}$ in terms of the volume V_T of a tetrahedron made by the six angular momentum quantum numbers. By using the Cayley-Menger determinant to calculate this volume, one gets for arbitrary transitions that

$$\begin{aligned} \lim_{\substack{n \rightarrow \infty \\ L/n < \infty}} \pi n^3 \left\{ \begin{matrix} \ell' & \ell & L \\ j & j & j \end{matrix} \right\}^2 &= \lim_{\substack{n \rightarrow \infty \\ L/n < \infty}} \left(2/n^6 \begin{vmatrix} 0 & 1 & 1 & 1 & 1 \\ 1 & 0 & j^2 & j^2 & j^2 \\ 1 & j^2 & 0 & \ell^2 & \ell'^2 \\ 1 & j^2 & \ell^2 & 0 & L^2 \\ 1 & j^2 & \ell'^2 & L^2 & 0 \end{vmatrix} \right)^{-1/2} \\ &= \frac{1}{\sqrt{\sin(\eta_1 + \eta_2)^2 - (L/n)^2}} \frac{1}{\sqrt{(L/n)^2 - \sin(\eta_1 - \eta_2)^2}} \end{aligned} \quad (12)$$

Here the limit is taken such that the ratio L/n remains finite, as well as the ratios for the initial and final angular momenta defined through $\cos\eta_1 = \ell/n$ and $\cos\eta_2 = \ell'/n$. This classical limit is valid only for values that make the arguments of the square root positive, which limits the integration range in L/n . For example, $L/n > \sin(\eta_1 - \eta_2)$, which depends on the change $\Delta\ell$ of angular momentum in transition.

The generalized character function H_{jL} is the solution of a differential equation that can be interpreted as Schrödinger's equation for a particle confined by a $1/\sin^2\chi$ potential well, that has infinite barriers at $\chi = 0$ and $\chi = \pi$

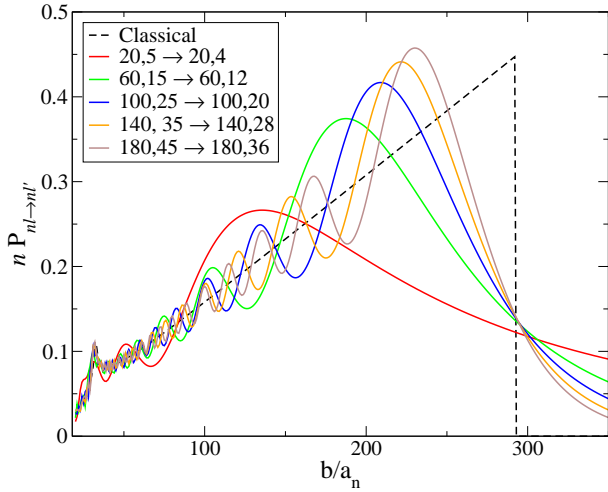


Figure 1. The convergence of quantum results toward the semi-classical limit, as expected from the correspondence principle. The parameters are chosen such that the ratios ℓ/n and ℓ'/n are preserved in all examples. The probabilities are also scaled by n to obtain the semi-classical limit which obeys the classical scaling. Here $a_n = n^2 a_0$.

and a minimum at $\chi = \pi/2$. A WKB approximation for this problem is obtained as

$$\lim_{\substack{n \rightarrow \infty \\ L/n < \infty}} H_{jL}(\chi) = \frac{1}{\sqrt{2 \sin \chi}} (\sin^2 \chi - (L/n)^2)^{-1/4} \quad (13)$$

and is in excellent agreement with the exact solution at any χ , except at the classical turning points ($|\sin \chi| = L/n$) where the WKB approximation diverges, showing that classically the particle tends to be found with infinite probability at the turning points. Beyond the turning points, the classical probability is zero while the exact solution decreases to zero gradually. This contradictory behavior is characteristic to the WKB approximation, and leads in the present case to a discontinuity in the transition probability as a function of b , as shown in Figures 1 and 2. The nature of this discontinuity is discussed below.

Figure 1 demonstrates graphically that probability (4) converges to (11) in the $n \rightarrow \infty$ limit, showing a linear increase up to a maximum impact parameter, followed by a sharp drop.

By combining equations (12) and (13), we see that classical probability is nonzero only when $\sin \chi < L/n < |\sin(\eta_1 - \eta_2)|$. Otherwise, integration (11) has analytic results in terms of elliptical integrals (see VOS12 for details). It is interesting to note that the same result was obtained directly from the classical solution of the motion under potential (1) and by defining the transition probabilities as ratios of phase space volumes (Vrinceanu & Flannery 2000). The resulting classical limit agrees very well with the non-perturbative result (4) as seen in the inset in Fig 2, for all b , except at very large b , where the probability drops to zero abruptly, instead of showing the $1/b^2$ decay of (2).

For $1 \ll b < b_{max}$, which means small α and χ , only small angular momentum changes are possible and one can approximate $\sin \chi \approx 2\alpha$, $\sin(\eta_1 - \eta_2) \approx \Delta\ell/\sqrt{n^2 - \ell^2}$ and $\sin(\eta_1 + \eta_2) \approx 2\ell\sqrt{n^2 - \ell^2}/n^2$, to provide a much simplified

transition probability

$$P_{nl \rightarrow n'l'}^{(C)} = \begin{cases} b/2b_{max} & \text{for } b \leq b_{max}/\Delta\ell \\ 0 & \text{for } b > b_{max}/\Delta\ell \end{cases} \quad (14)$$

where the classical cutoff radius $b_{max} = 3na_0\sqrt{n^2 - \ell^2}Ze^2/\hbar v$ is obtained from the cusp relation $\sin \chi = |\sin(\eta_1 - \eta_2)|$. This linear increase for $b < b_{max}$ is in contrast with the *ad-hoc* PS64 assumption that the probability is $1/2$ for $b < R_1$, and it explains why the PS64 rate coefficient is larger than the quantum VOS12 rate coefficient.

The abrupt discontinuity in b at b_{max} displayed by equation (14) is problematic, reflecting the deficiency of the WKB approximation to describe quantum tunneling. The most significant difficulty for (14) is for dipole allowed $|\Delta\ell| = 1$ transitions that have logarithmically divergent cross sections. Instead, by using probability (14) in integrating (3) the result is a finite cross section, denoted as σ_C for future reference. For all other $|\Delta\ell| > 1$ transitions, the sharp discontinuity has a minor effect since both the classical and quantum transitions have finite cross sections and rate coefficients, and the approximation (14) works surprisingly well. The next section shows how to address the deficiency of classical probability (14) for $\Delta\ell = 1$ at $b = b_{max}$ by taking the classical limit differently. This procedure is akin to the textbook prescription of treating the WKB singularity at the turning points, by developing a local approximation around those points and then "stitching" together approximations over various intervals.

5 SEMICLASSICAL LIMIT

Instead of the classical approximation (13) valid over a wide range of χ values, we use a local approximation (Varshalovich 1988)

$$\lim_{\substack{n \rightarrow \infty \\ \alpha \rightarrow 0, \alpha n < \infty}} \frac{1}{n} H_{jL}(\chi) = j_L(2\alpha n) \quad (15)$$

valid only for small α , as long as the product αn is finite. Here $j_L(x)$ is the spherical Bessel function.

By using this approximation in the integration (11), and working only for dipole transitions $\ell' = \ell \pm 1$, we obtain a semiclassical transition probability as the integral

$$P^{(SC)} = \frac{2\ell}{\pi} \int_1^n \frac{j_L^2(n\alpha) dL}{\sqrt{4\ell^2[1 - (\ell/n)^2] - L^2}} \quad (16)$$

which is dominated by values around the $L = 1$ end of the integration range. Since $j_1(x) \approx x/3 + \mathcal{O}(x^3)$, this semiclassical transition probability has the correct asymptotic $\sim 1/b^2$ at $b \rightarrow \infty$ limit. The integral can be approximated to get

$$P^{(SC)} \approx \frac{3}{2} j_1^2(2\alpha\sqrt{n^2 - \ell^2}) \quad (17)$$

Figure 2 shows the PS64 perturbation theory (2), classical approximation (14) and semiclassical approximation (17) for a dipole allowed transition as compared with the quantum probability (4). The classical limit agrees well with the exact result for low and moderate impact parameters (as shown in inset), displaying the abrupt classical discontinuity at b_{max} . On the other hand, the semiclassical approximation does well at very large b , but fails at small $b < b_S$, as shown in the figure by a dashed line.

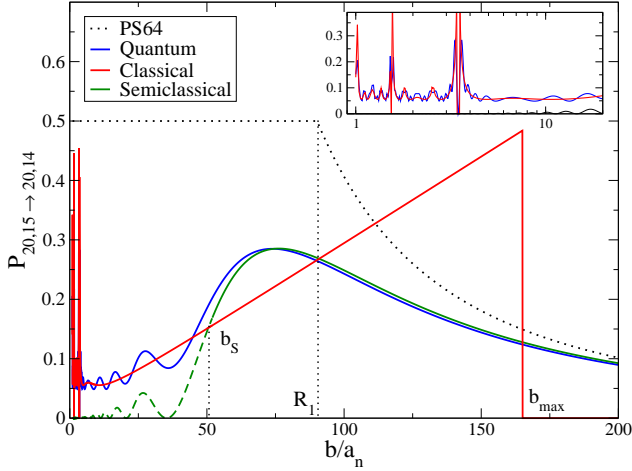


Figure 2. Probability for transitions within the $n = 20$ hydrogenic shell from $\ell = 15$ to $\ell' = 14$ in collisions with protons having speed $v = 0.25v_n$ as a function of scaled impact parameter. The quantum theory is contrasted with the classical and semiclassical approximations and with the perturbative result in Equation (2). We observe that the PS-M model (Guzmán et al. 2017) brings the results to better agreement with quantum results than PS64. The inset shows the good agreement between the classical approximation and the quantum result at small impact parameter.

In order to take advantage of the good agreement of the classical and semiclassical transition probabilities in their respective ranges and obtain an accurate approximation for the cross section, we combine them in an *effective* transition probability defined as:

$$P_{n\ell \rightarrow n\ell'}^{(E)} = \begin{cases} b/2b_{\max} & \text{for } b \leq b_S \\ \frac{3}{2}j_1^2(b_{\max}/b) & \text{for } b > b_S \end{cases} \quad (18)$$

with the matching $b_S = \gamma b_{\max}$ defined as the smallest impact parameter for which the classical and semiclassical approximations are equal, ensuring the continuity of the probability, and $\gamma = 0.3235133$ is the solution to the transcendental equation $j_1^2(1/x) = x/3$.

The cross section is calculated by using Eq. (3) to get the semiclassical cross section

$$\sigma_{n\ell \rightarrow n\ell'}^{(SC)} = \frac{\pi b_{\max}^2}{3} \begin{cases} (R_c/b_{\max}^2)^3 & , R_c \leq b_S \\ \gamma^3 + [T(R_c/b_{\max}) - T(\gamma)] & , R_c > b_S \end{cases} \quad (19)$$

where the function T is

$$T(x) = -Ci(2/x) + 3 * x^4(3 + 2x^2)/8 - x^2(2 - 3x^2 + 6x^4) \cos(2/x)/8 + x(2 - x^2 - 6x^4) \sin(2/x)/4 \quad (20)$$

and $Ci(z) = -\int_z^\infty \cos(t)/t dt$ is the cosine integral function.

Figure 3 shows calculations of the cumulative transition cross section as a function of the cutoff parameter R_c used to regularize the logarithmic singularity. The PS64 result overestimates the non-perturbative quantum cross section derived from Eq. (4) by amounts that depend on the cutoff parameter R_c . As explained in section 2, the PS64 rates are overestimated because the probability of transition is assumed to be 1/2 for $0 < b < R_1$, while the non-perturbative calculation demonstrates that the probability

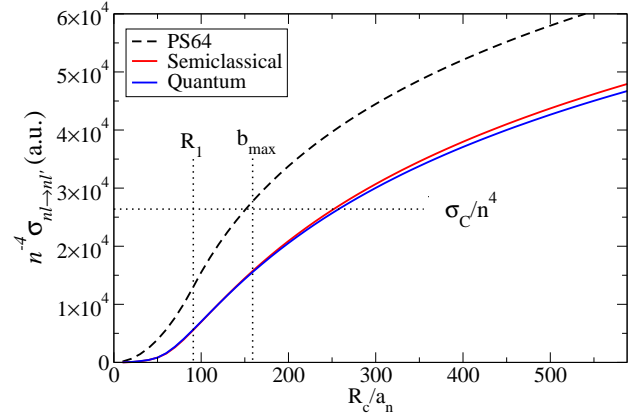


Figure 3. The cumulative cross section $\sigma_{\ell \rightarrow \ell'}$ in atomic units as a function of the scaled cutoff parameter R_c for the exact quantum theory, its semiclassical limit and for the PS64 perturbative approximation. The plot shows the $(20,15) \rightarrow (20,14)$ transition in collisions with ions with speed $v = 0.25v_n$. The corresponding scaled finite classical cross section σ_C is marked on the graph. The low b cutoff R_1 used by PS64 and the b_{\max} impact parameter after which the classical transition probability is zero, are shown as dotted lines.

increases linearly with b . Asymptotically, both PS64 and the semiclassical cross sections (19) diverge logarithmically as $\sim \text{const} + \pi b_{\max}^2 \ln(R_c)/3$ with $R_c \rightarrow \infty$, but with the PS64 constant approximately twice as large as the semiclassical one. Therefore, even for high temperature and density considered by Guzmán et al. (2016, 2017) the PS64 rate overestimates the ℓ -changing rate by a constant amount. This difference is independent of R_c , and therefore the ratio of the two rates approaches unity in the $R_c \rightarrow \infty$. The PS-M model also has the linear increase with b and the same asymptotic behavior, but as noted in their paper, the agreement with the quantum VOS12 model is reasonable good in general, similar with the results derived from Eq. (18), but deficient in some extreme cases, such as low ℓ values.

Recent papers (Guzmán et al. 2016, 2017; Williams et al. 2017) argued that quantum formula (4) is computationally expensive, while the classical limit (14) has an abrupt drop, instead of the $1/b^2$ decay as $b \rightarrow \infty$, and therefore the PS64 perturbative rates should be still preferable. Figure 3 addresses this concern by showing that semiclassical cross sections, and by extension the transition rate coefficients, are consistent with quantum non-perturbative results, but easier to use in practical calculations due to the simplicity of the effective probability (18).

6 CONCLUSIONS

We have contrasted two different models for the evaluation of proton-Rydberg atom angular changing collision, with particular emphasis on the anatomy of their assumptions and approximations, and the comparison to the full quantum-mechanical setting at small principal quantum numbers.

We argue that parameters of astrophysical interest derived from diverging cross-sections contain a degree of arbitrariness in principle reflected in large and unknown systematic errors. In the absence of full quantum calculations or of precision laboratory measurements, it is more meaningful to use models with clearer physical interpretation, less assumptions, and controllable approximations. We believe that this pluralistic approach is even more imperative in astrophysics, since the models involved in the extraction of astrophysical parameters from observations are typically the major source of systematic error, as already extensively advocated in Mashonkina (1996, 2009); Bergemann (2010); Hillier (2011).

It was advocated in Guzmán et al. (2016, 2017) that VOS12 quantum rates to be used when high accuracies are required and faster PS64 when that accuracy is not needed to speed the calculations. The results introduced here, derived from improved semiclassical limit (18), are accurate over the whole range of impact parameters and computationally inexpensive, eliminating the dilemma of having to choose speed over accuracy.

ACKNOWLEDGMENTS

This work was supported by the National Science Foundation through a grant to ITAMP at the Harvard-Smithsonian Center for Astrophysics. One of the authors (DV) is also grateful for the support received from the National Science Foundation through grants for the Center for Research on Complex Networks (HRD-1137732), and Research Infrastructure for Science and Engineering (RISE) (HRD-1345173). We thank G. Ferland, and his collaborators, for fruitful and stimulating dialog on this topic.

REFERENCES

- Bellomo P., Stroud C. R., Farrelly D., T. Uzer, 1998, Phys. Rev. A, 58, 3896
- Benjamin R. A., Skillman E. D., Smits D. P., 1999, ApJ, 514, 307
- Benjamin R. A., Skillman E. D., Smits D. P., 2002, ApJ, 569, 288
- Bergemann M., 2010, *Uncertainties in Atomic Data and How They Propagate* in Chemical Abundances, ed. V. Luridiana, J. Garcías Rojas, & A. Manchado (Instituto de Astrofísica de Canarias), (arXiv:1104.1640)
- Bray I., Stelbovics A. T., 1992, Phys. Rev. A, 46, 6995
- Brocklehurst M., 1970, MNRAS, 148, 417
- Chluba J., Rubiño-Martin J. A., Sunyaev R. A., 2007, MNRAS, 374, 1310
- Chluba J., Vasil G. M., Dursi L. J., 2010, MNRAS, 407, 599
- Ferland G. J., 1986, ApJ, 310, L67
- Gabrielse G., 2005, Adv. At. Mol. Opt. Phys., 50, 155
- García-Rojas J., Esteban C., 2007, ApJ, 670, 457
- Guzmán F., et al., 2016, MNRAS, 459, 3498
- Guzmán F., et al., 2017, MNRAS, 464, 312
- Hillier, D.J., 2011, Ap&SS, 336, 87
- Izotov Y. I., Stasińska G., Meynet G., Guseva N. G., Thuan T. X., 2006, A&A, 448, 955
- Izotov Y. I., Thuan T. X., Stasińska G., 2007, ApJ, 662, 15
- Luridiana V., Peimbert A., Peimbert M., Cerviño M., 2003, ApJ, 592, 846
- Mashonkina, L.I., 1996, in ASP Conf. Ser. 108, Model Atmospheres and Spectrum Synthesis, ed. S.J. Adelman, F. Kupka, & W.W. Weiss (San Francisco, CA:ASP), 140
- Mashonkina, L., 2009, Phys. Scr., T 134, 014004
- Nicholls D. C., Dopita M. A., Sutherland R. S., 2012, ApJ, 752, 148
- Otsuka M., Meixner M., Riebel D., et al., 2011, ApJ, 729, 39
- Pengelly R. M., Seaton M. J., 1964, MNRAS, 127, 165
- Pipher J. L., Terzian Y., 1969, ApJ, 155, 165
- Pohl T., Vrinceanu D., Sadeghpour, H.R., 2008, Phys. Rev. Lett., 100, 223201
- Ponzano G., Regge T., 1968, *Spectroscopic and Group Theoretical Methods in Physics* Block, F. (ed.). New York, pp 1-58
- Presnyakov L. P., Urnov A. M., 1970, J. Phys. B, 3, 1267
- Samuelson R. E., 1970, J. Atmos. Sci., 27, 711
- Storey P. J., Sochi T., 2015, MNRAS, 446, 1864
- Sun X., D., McAdams K. B., 1993, Phys. Rev. A, 47, 3913
- Varshalovich D. A., Moskalev A. N., Khersonskii V. K., 1988, *Quantum Theory of Angular Momentum*, World Scientific (Singapore), 109
- Vrinceanu D., Flannery M.R., 2000, Phys. Rev. Lett., 85, 4880
- Vrinceanu D., Flannery M.R., 2001, Phys. Rev. A, 63, 032701
- Vrinceanu D., Flannery M.R., 2001, J. Phys. B, 34, L1
- Vrinceanu D., Onofrio R., Sadeghpour, H. R., 2012, ApJ, 747, 56
- Vrinceanu D., Onofrio R., Sadeghpour, H. R., 2014, ApJ, 780, 2
- Williams R. J. R., et al., 2017, J. Phys. B, 50, 115201

This paper has been typeset from a $\text{\TeX}/\text{\LaTeX}$ file prepared by the author.